ArXiv: astro-ph, Nov 16-21, 2015

от Сильченко О.К.

Astro-ph: 1511.04442

How to bend galaxy disc profiles II: stars surfing the bar in anti-truncated discs

J. Herpich[1⋆†], G. S. Stinson[1], H.-W. Rix[1], M. Martig[1], A. A. Dutton[1]
[1] *Max-Planck-Institut für Astronomie, Königstuhl 17, 69117, Heidelberg, Germany*

17 November 2015

ABSTRACT
Simple numerical models can produce the observed radial breaks in the stellar surface density profile of late-type galaxies by varying only one parameter, the initial halo spin λ. Here we analyse these simulations in more detail in an effort to identify the physical mechanism that leads to the formation of anti-truncations (Type-III profiles). We find that orbital resonances with a central bar drive stellar orbits from circular orbits with small semi-major axes to rather eccentric orbits with large semi-major axes. These orbits then form a disk-like configuration with high radial dispersion and rotation far below the circular velocity. This will manifest itself in photometry as an anti-truncated (Type-III) outer stellar disk. Whether such outer disks – with qualitatively new dynamics – exist in nature can be tested by future observations.

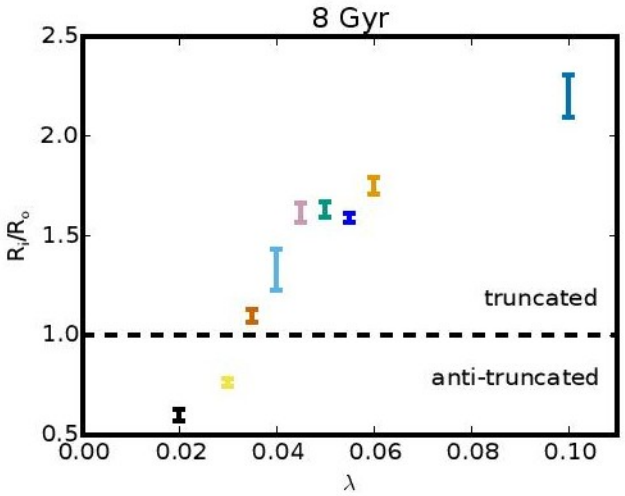

Figure 2. Ratios of inner to outer scale length as a function of spin parameter λ from broken exponential fits. The errorbars indicate the range between the 16-th and the 84-th percentile. The ratio is below unity (up-bending) for $\lambda \lesssim 0.03$, roughly unity (pure exponential) at $\lambda = 0.035$ and above unity (down-bending) for $\lambda \gtrsim 0.04$.

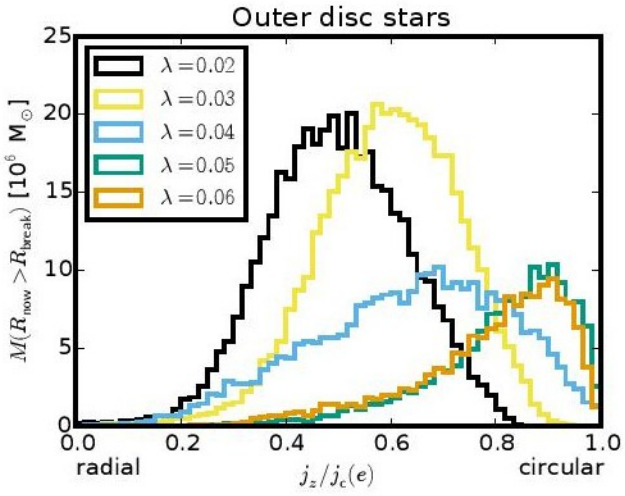

Figure 3. Circularity distribution in outer disc. The figure shows the circularity distribution of stars in the disc outskirts ($R > R_{\rm b}$) for a choice of simulations spanning the from the range from low ($\lambda = 0.02$) to high spins ($\lambda = 0.06$). Most orbits in the high spin simulations ($\lambda > 0.04$) are circular while there is not a single star with $\frac{j_z}{j_c(e)} \gtrsim 0.85$ in the lowest spin simulation. Intermedi-

Разница в радиальной и вертикальной дисперсии скоростей

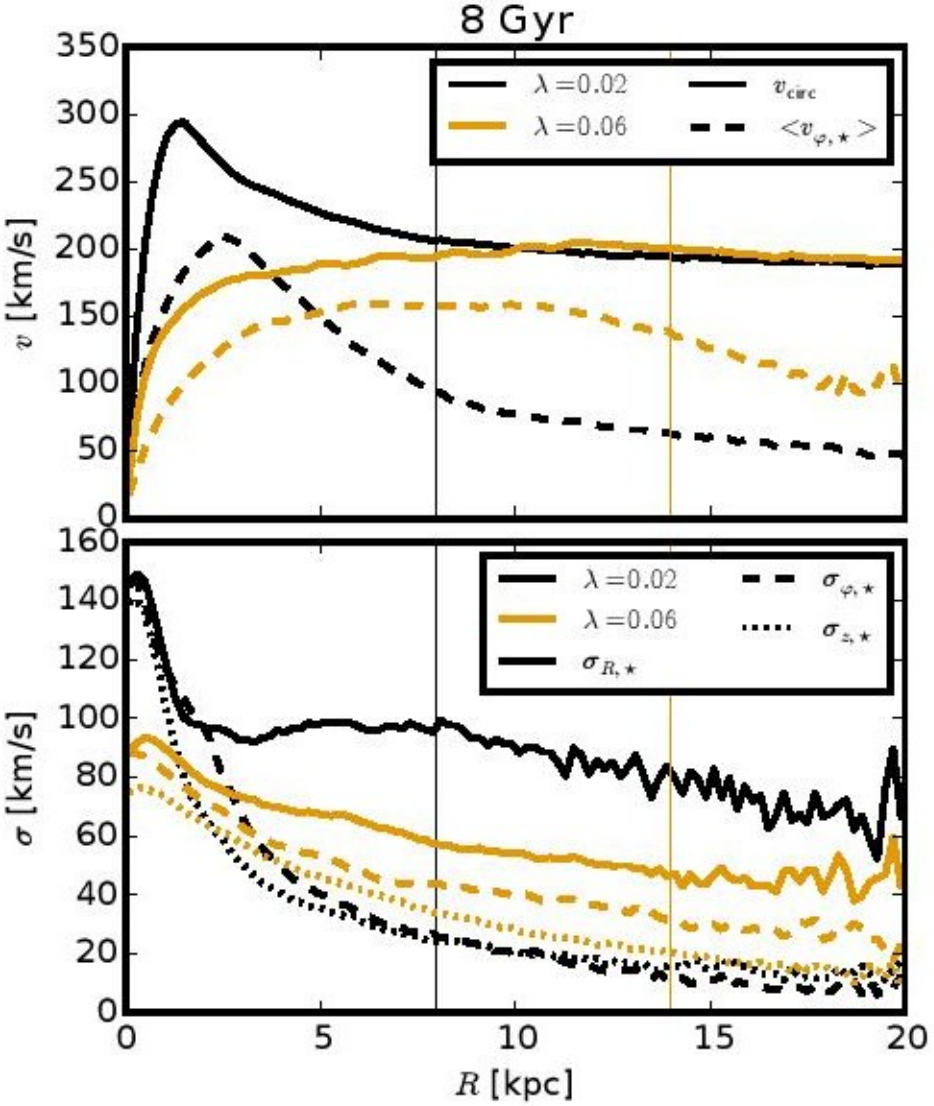

Astro-ph: 1511. 04455

A $5 \times 10^9\ M_\odot$ BLACK HOLE IN NGC 1277 FROM ADAPTIVE OPTICS SPECTROSCOPY

JONELLE L. WALSH[1], REMCO C. E. VAN DEN BOSCH[2], KARL GEBHARDT[3], AKIN YILDIRIM[2], DOUGLAS O. RICHSTONE[4], KA
GÜLTEKIN[4], AND BERND HUSEMANN[5]

[1] George P. and Cynthia Woods Mitchell Institute for Fundamental Physics and Astronomy, Department of Physics and Astronomy, Texas A&M Un
College Station, TX 77843, USA; walsh@physics.tamu.edu

[2] Max-Planck Institut für Astronomie, Königstuhl 17, D-69117 Heidelberg, Germany

[3] Department of Astronomy, The University of Texas at Austin, 2515 Speedway, Stop C1400, Austin, TX 78712, USA

[4] Department of Astronomy, University of Michigan, 1085 S. University Ave., Ann Arbor, MI 48109, USA

[5] European Southern Observatory, Karl-Schwarzschild-Str. 2, 85748 Garching, Germany

Draft version November 17, 2015

ABSTRACT

The nearby lenticular galaxy NGC 1277 is thought to host one of the largest black holes known, however the black hole mass measurement is based on low spatial resolution spectroscopy. In this paper, we present Gemini Near-infrared Integral Field Spectrometer observations assisted by adaptive optics. We map out the galaxy's stellar kinematics within ~440 pc of the nucleus with an angular resolution that allows us to probe well within the region where the potential from the black hole dominates. We find that the stellar velocity dispersion rises dramatically, reaching ~550 km s^{-1} at the center. Through orbit-based, stellar-dynamical models we obtain a black hole mass of $(4.9 \pm 1.6) \times 10^9\ M_\odot$ (1σ uncertainties). Although the black hole mass measurement is

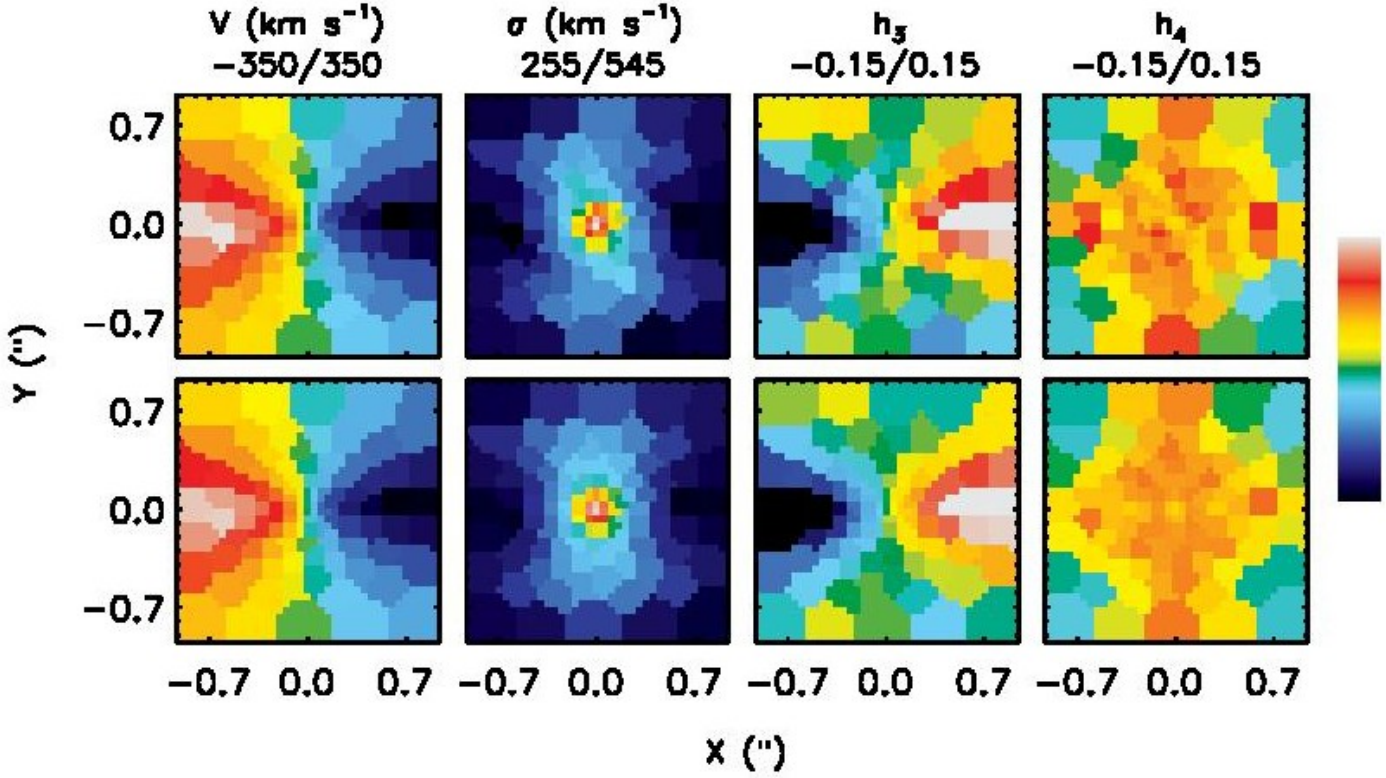

FIG. 3.— The observed NIFS kinematics (top) show that NGC 1277 is rotating, with the west side of the galaxy being blue-shifted, that there is a sharp rise in the velocity dispersion and generally positive h_4 values at the nucleus, and that h_3 and V are anti-correlated. The best-fit stellar dynamical model (bottom) is shown on the same scale given by the color bar to the right and the minimum/maximum values are provided at the top of the maps. The best-fit model nicely reproduces the NIFS observations and has a reduced χ^2 of 0.7.

Эффект пространственного разрешения

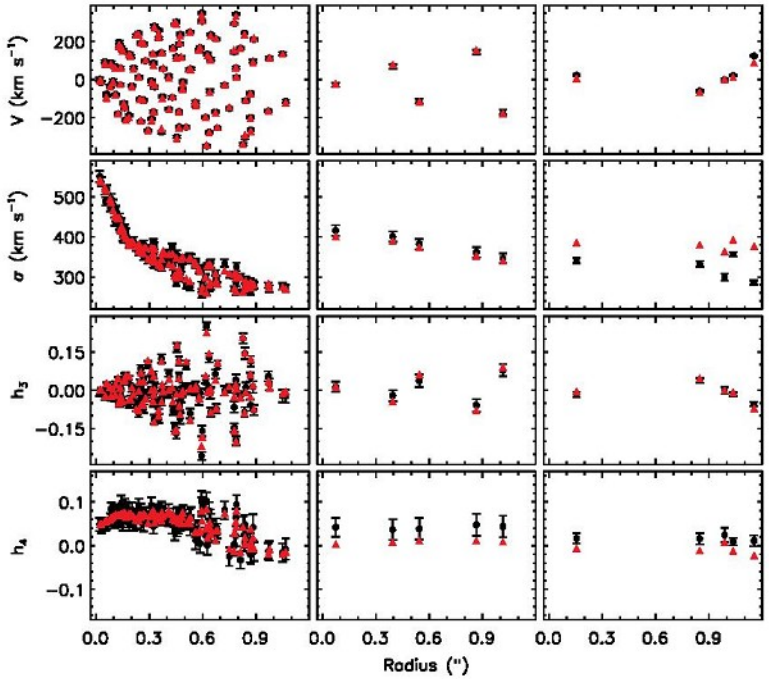

FIG. 4.— The observed kinematics (black circles) measured from NIFS (left column), HET (middle column), and PPAK (right column) are shown over the radial extent of the NIFS data. The data have been folded and are plotted as a function of projected distance from the nucleus. While the HET measurements have been made along the galaxy major axis, multiple position angles are depicted for the IFU data. For comparison, we plot the best-fit model constrained by only the NIFS kinematics (red triangles). Thus, the best-fit model predictions for the central HET and PPAK kinematics take into account differences in spatial resolution.

Положение на шкалирующих диаграммах

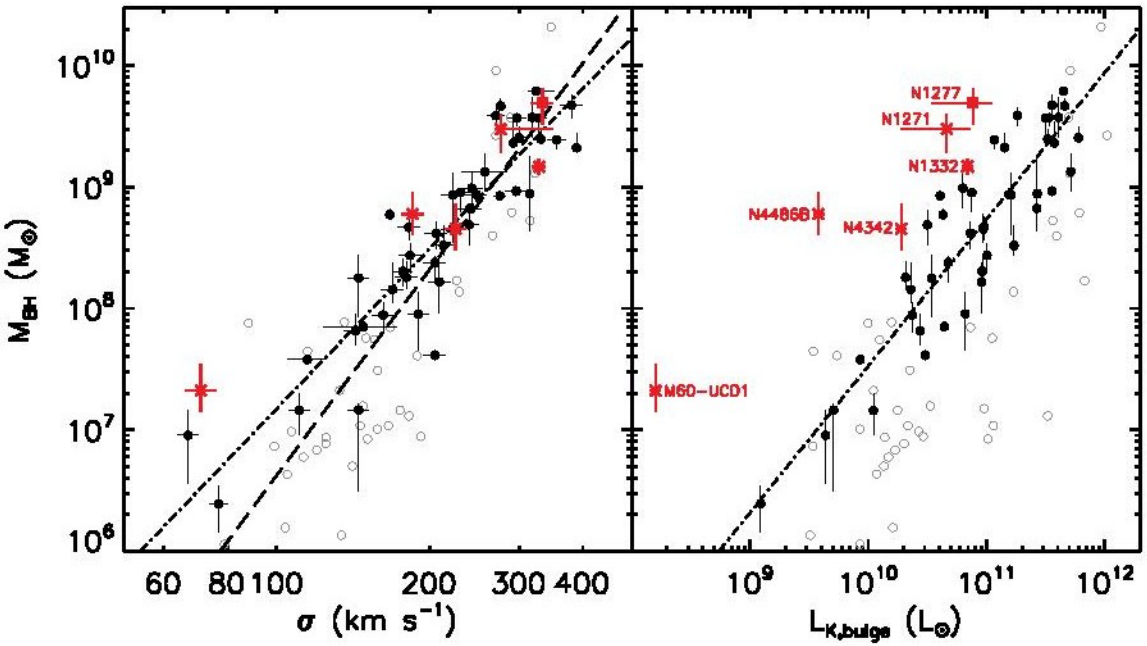

FIG. 5.— The location of NGC 1277 (red square) and other similar galaxies (red asterisks) on the black hole–host galaxy correlations. The ∼80 galaxies with dynamical black hole mass measurements shown here are taken from Kormendy & Ho (2013), with the exception of M60-UCD1 (Seth et al. 2014), NGC 1332 (Rusli et al. 2011), NGC 1271 (Walsh et al. 2015), and NGC 1277 (this work). The dot-dashed lines show the fitted relations from Kormendy & Ho (2013) to the black points. The gray points, composed largely of galaxies with pseudo-bulges, were excluded from the Kormendy & Ho (2013) fit. For comparison, the steeper dashed line is the relation from McConnell & Ma (2013), which was fit to nearly all points. NGC 1277 and the galaxies labeled in red have small sizes and large velocity dispersions for their galaxy luminosities, and they harbor over-massive black holes relative to $M_{\rm BH} - L_{\rm bul}$ but are consistent with the $M_{\rm BH} - \sigma_\star$ relation.

Astro-ph: 1511.05654

Explaining the reportedly over-massive black holes in early-type galaxies with intermediate-scale discs

Giulia A. D. Savorgnan[1]⋆, Alister W. Graham[1]

[1] *Centre for Astrophysics and Supercomputing, Swinburne University of Technology, Hawthorn, Victoria 3122, Australia.*

Варианты декомпозиции профиля яркости

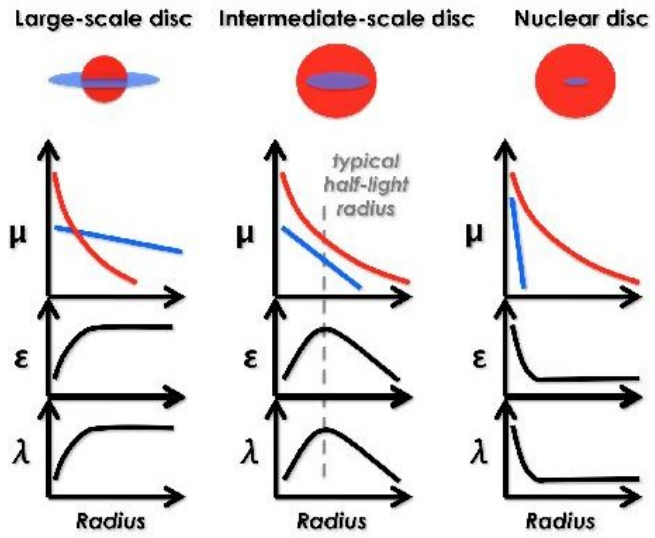

Figure 1. Illustration of the spheroid/disc decomposition of the one-dimensional surface brightness profile, μ, the ellipticity profile, ϵ, and the specific angular momentum profile, λ, for the three prototype early-type galaxy sub-classes. In the flux decompositions, the spheroid (or bulge) and the disc are shown with the red and blue color, respectively. The left panel shows a disc-dominated central fast rotator (lenticular galaxy), composed of a bulge encased in a large-scale disc. The right panel displays a spheroid-dominated slow rotator (elliptical) with (an op-

Примеры тех самых S0…

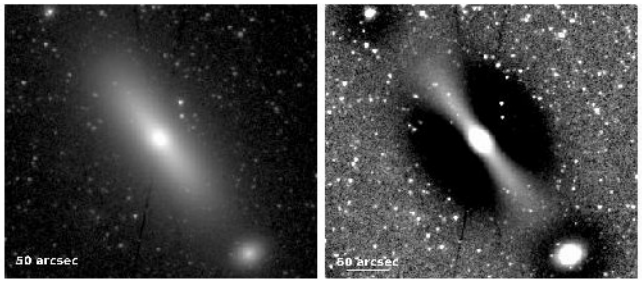

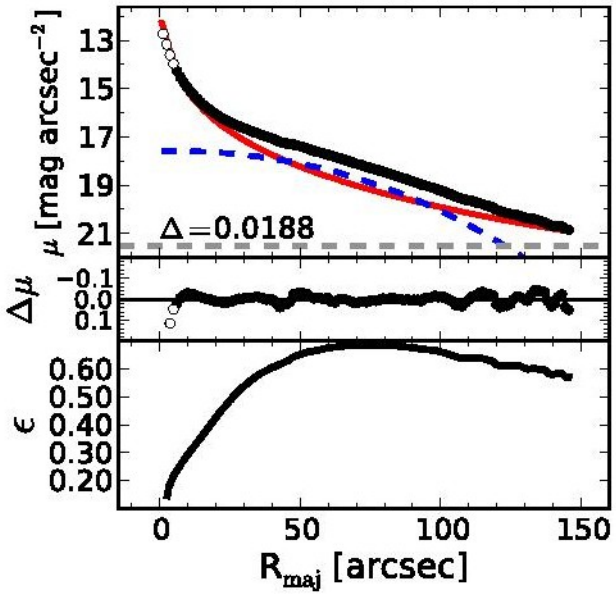

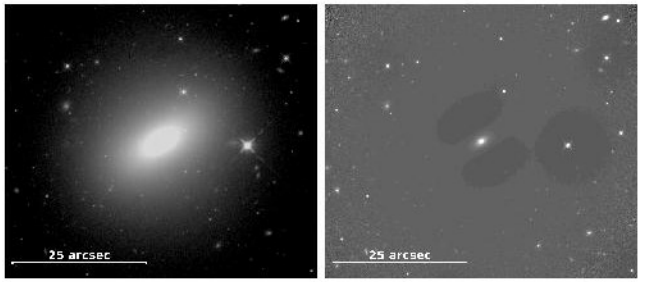

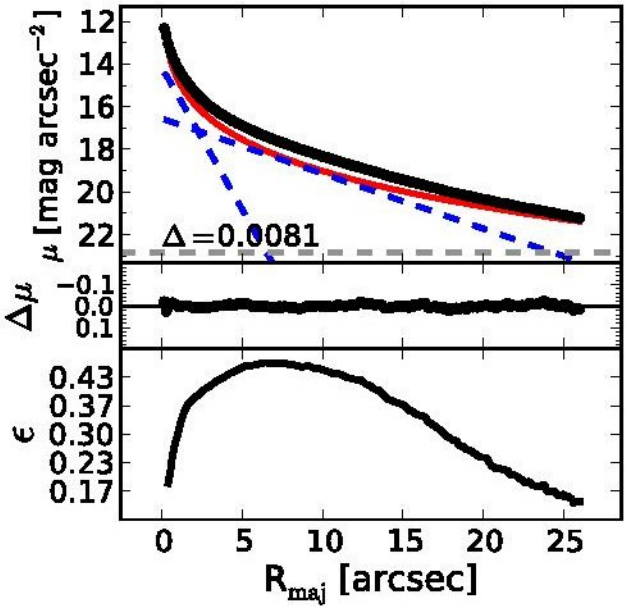

Astro-ph: 1511.05572

Establishing the level of cylindrical rotation in Boxy/Peanut bulges

A. Molaeinezhad[1⋆], J. Falcón-Barroso[2,3], I. Martínez-Valpuesta[2,3], H.G. Khosroshahi[1], M. Balcells[2,4], and R.F. Peletier[5]

[1]*School of Astronomy, Institute for Research in Fundamental Sciences (IPM), PO Box 19395-5746 Tehran, Iran*
[2]*Instituto de Astrofísica de Canarias, E-38200, La Laguna, Spain*
[3]*Depto. Astrofísica, Universidad de La Laguna (ULL), E-38206 La Laguna, Tenerife, Spain*
[4]*Isaac Newton Group of Telescopes, Apartado 321, 38700 Santa Cruz de La Palma, Canary Islands, Spain*
[5]*Kapteyn Astronomical Institute, University of Groningen, Postbus 800, 9700 AV Groningen, the Netherlands*

Accepted 2015 November 16. Received 2015 November 05; in original form 2015 July 07

ABSTRACT

We present SAURON integral-field observations of a sample of 12 mid to high-inclination disk galaxies, to unveil hidden bars on the basis of their kinematics, i.e., the correlation between velocity and h_3 profiles, and to establish their degree of cylindrical rotation. For the latter, we

Выборка

Table 1. Basic properties of our sample of galaxies

Galaxy	V_{LG} (kms^{-1})	Scale $(kpc/'')$	B/D	Inclniation (deg)	Type $(RC3)$	Type $(Buta+2015)$	PA $(deg$
(1)	(2)	(3)	(4)	(5)	(6)	(7)	(8)
NGC 0678	3015	0.19	-	82	$SB(s)b\ sp$	$SAB(s,nd)a\ sp$	9
NGC 5326	2596	0.17	0.73	65	$SAa?$	$E(d)5/S0\ sp$	-138
NGC 5422	1977	0.13	1.28	90(90)	$S0\ sp$	$SAB_{ax}0^o\ sp/E(d)8$	64
NGC 5475	1815	0.12	0.14	78(79)	$Sa?\ sp$	-	-101
NGC 5689	2295	0.15	0.89	81	$SB(s)0/a$	$(R'L)SAB:(r'l,nd)0^+\ sp$	-5
NGC 5707	2358	0.15	0.42	80	$Sab?\ sp$	$SA0^o\ sp$	-59
NGC 5746	1680	0.12	0.68	81	$SAB(rs)b?\ sp$	$(R')SB_x(r,nd)0/a\ sp$	-99
NGC 5838	1316	0.09	0.71	72	$SA0^-$	-	134
NGC 5965	3603	0.23	0.53	80	Sb	-	-38
NGC 6010	2036	0.14	0.27	84(90)	$S0/a?\ sp$	$SA(l)0^o\ sp$	12
NGC 7332	1481	0.08	0.41	81(84)	$S0\ pec\ sp$	-	-114
NGC 7457	1134	0.06	10.0	70(74)	$SA0^-(rs)?$	-	35

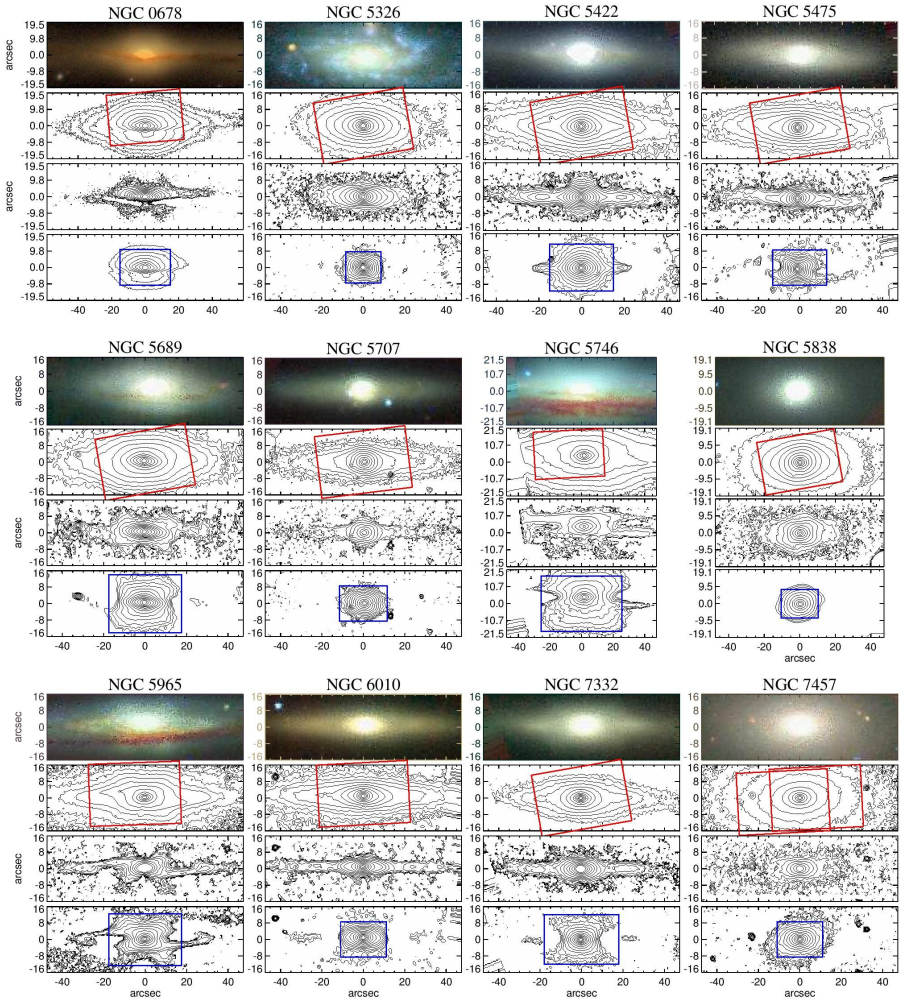

Figure 2. U-R-K composite images, Isophotes and unsharp masks for all 12 galaxies in our sample. For each galaxy, First panel: The U-R-K composite image, from Peletier & Balcells (1997) . U– and R-band images were obtained with the Prime Focus camera of the Isaac Newton telescope and K -band images were taken at the UK infrared telescope (UKIRT), using the IRCAM3 Camera. For NGC 0678 we have used Sloan Digital Sky survey DR10 data. Second panel: Isophotes of the K-band images. The SAURON final pointing is shown on top of this panel. Third panel: Unsharp masked K-band image. The unsharp masking technique allows us to highlight the structure of the galaxy in more details, for instance, the X-shape bulge is clearly visible for 6 galaxies in our sample (NGC 0678, NGC 5422, NGC 5689, NGC 5746, NGC 5965 and NGC 7332). Fourth Panel: Isophotes of the K-band image, after subtracting an exponential disk from the observed image. We have used the disk-subtracted images together with the unsharp masked galaxy images (third panel) to have a rough estimation of bulge size in the (x, z) space. This analysis bulge window is shown as a blue rectangle on top this panel.

Метод «цилиндричности вращения»

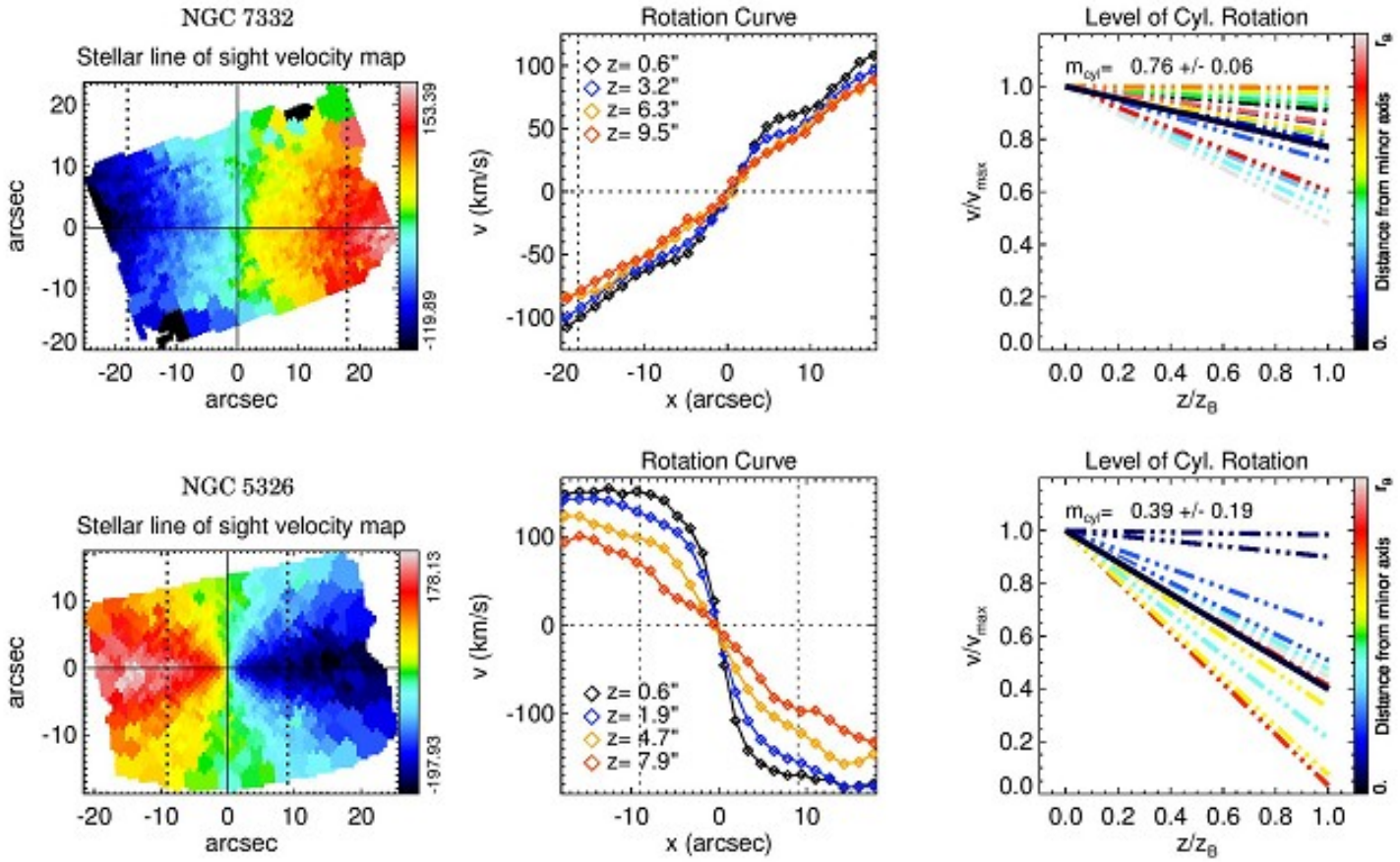

Figure 4. (*Left*) The velocity map of NGC 7332 (a cylindrical rotating system) and NGC 5326 (a non cylindrical rotator). In these plots, velocity maps are rotated so that the horizontal axis is parallel to the major axis of the galaxies. Vertical dotted lines mark the bulge boundaries. (*Middle*) The stellar line of sight velocity parallel to the major axis of galaxies at different height (z) from the disk plane. (Right) Line-of-sight velocity gradient along the minor axis of galaxies at different distance from the minor axis. Profiles are color-coded according to the distance from the minor axis. Solid black profile represents the average value. We define $m_{\rm cyl} = m_{\rm avg} + 1$ as a quantity to express the level of cylindrical rotation, in which $m_{\rm avg}$ is the slope of the solid black line . See text for the definition of the various quantities $m_{\rm cyl}$, z_B and V_{max}.

Теория

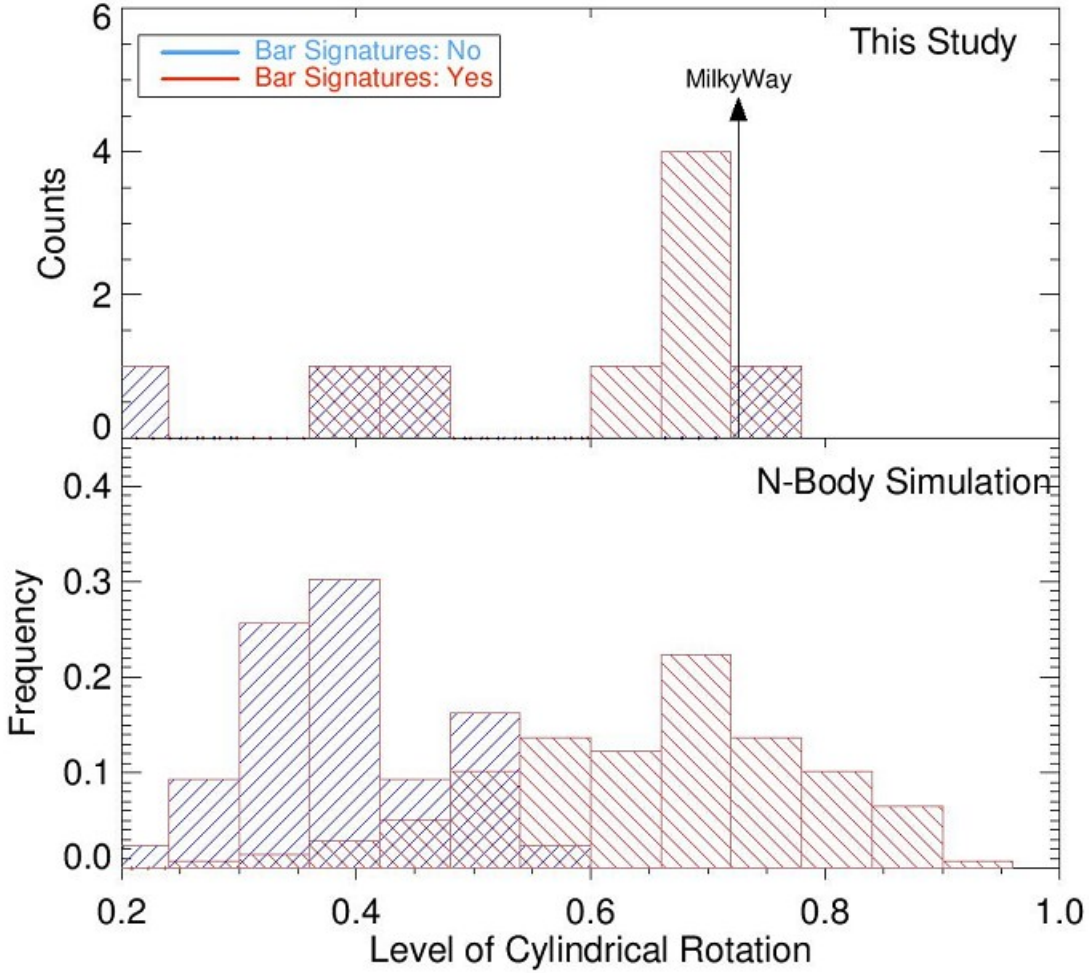
Bar Signatures: No
Bar Signatures: Yes
This Study
MilkyWay
Counts
N-Body Simulation
Frequency
Level of Cylindrical Rotation

Результаты

NGC number	**0678**	**5326**	**5422**	**5475**	**5689**	**5707**	**5746**	**5838**	**5965**	**6010**
1) Double-hump rotation curve	Y	N	Y	N	Y	N	Y	Y	Y	N?
2) Broad central σ peak with plateau at moderate radii	N?	N	N?	N	Y	N	Y	Y	Y	N
3) $V - h_3$ correlation over the projected bar length	Y	N	Y	N	Y	N	Y	Y	Y	N
Central $V - h_3$ anti-correlation	Y	N	Y	Y	Y	N	Y	Y	Y	Y
Boxy/Peanut Bulge	Y	N	Y	N	Y	N	Y	N	Y	N
Degree of Cyl. Rotation ($m_{\rm cyl}$)	0.66 ± 0.09	0.39 ± 0.19	0.70 ± 0.07	0.44 ± 0.17	0.64 ± 0.09	0.22 ± 0.21	0.63 ± 0.08	0.40 ± 0.17	0.62 ± 0.10	0.42 ± 0.17
Bar	Y	N	Y	N	Y	N	Y	Y	Y	Y?